ISSN 0915-633X

NATIONAL INSTITUTE FOR FUSION SCIENCE

Comparison of Parallel Viscosity with Neoclassical Theory

K. Ida and N. Nakajima

(Received - Mar. 12,1996)

NIFS-411 Apr. 1996

RESEARCH REPORT
NIFS Series

NAGOYA, JAPAN

Comparison of parallel viscosity with neoclassical theory

K.Ida, N.Nakajima

National Institute for Fusion Science

Nagoya 464-01 Japan

Abstract

Toroidal rotation profiles are measured with charge exchange spectroscopy for the plasma heated with tangential NBI in CHS heliotron/torsatron device to estimate parallel viscosity. The parallel viscosity derived from the toroidal rotation velocity shows good agreement with the neoclassical parallel viscosity plus the perpendicular viscosity. ($\mu_{\perp}=2m^2/s$).

Keywords : Charge exchange spectroscopy, Heliotron/torsatron, Neoclassical parallel viscosity

In heliotron/torsatron devices, because of non axis-symmetry of magnetic field, the parallel viscosity causes the damping of toroidal rotation velocity. The toroidal rotation profiles are measured using charge exchange spectroscopy[1] and the magnitude of parallel viscosity has been compared with the preliminary neoclassical calculations in the high aspect ratio limit[2] in Compact Helical System (CHS)[3]. In this brief communication, neoclassical parallel viscosity is calculated more precisely by including the three dimensional magnetic structure[4].

CHS is a heliotron/torsatron device (poloidal period number l = 2, and toroidal period number m = 8) with a major radius (R) of 95 cm and an average minor radius (a) of 20 cm. The magnetic field ripple on the inboard side (R=90-95cm) is negligible, however, it increases sharply for R >95 cm and reaches 8 % at R = 101.6 cm. Therefore the magnetic field ripple at the plasma center can be modified from zero to 8% by shifting the magnetic axis R_{ax} from 89.9cm to 101.6cm and the damping of toroidal rotation due to TTMP can be studied.

Figure 1 shows toroidal rotation velocity profiles as a result of a major radius scan (R_{ax}=89.8, 94.9, 97.4cm), which is controlled by the vertical field strength in CHS heliotron/torsatron. The plasma is produced initially by electron cyclotron heating (ECH) in hydrogen gas and sustained with tangential NBI (absorbed power of 0.5 MW in the direction parallel to the helical current). The line-averaged density reaches about 2 x 10^{13} cm^{-3} after NB injection.

As is well known, in axisymmetric systems, the direction of the flow to be damped by the parallel viscosity is determined by the symmetry, i.e., the flow in the direction without symmetry (poloidal flow) is damped. Thus, the viscosity coefficient appears in the expression of the parallel viscosity in order to determine the magnitude of the damping.On the other hand, in non-axisymmetric systems, both the direction and the magnitude of the damping should be specified. Therefore the parallel viscosity neglecting the heat flux can be expressed as[4)]

$$\langle \vec{B} \cdot \nabla \cdot \pi_a \rangle = \mu_a \langle \vec{U}_a \cdot \nabla \theta_a^* \rangle \tag{1}$$

where μ_a is the viscosity coefficient mainly determining the magnitude of the damping and θ_a^* is a angle-like variable mainly determining the direction of the damping :

$$\theta_a^* \equiv (I + \langle G_{BS} \rangle_a)\theta + (J - \tau \langle G_{BS} \rangle_a)\phi \tag{2}$$

with the poloidal (toroidal) angle $\theta(\phi)$ in the Boozer coordinate system, the poloidal (toroidal) current outside (inside) of the flux surface $2\pi J$ $(2\pi I)$, the rotational transform τ, and the geometric factor $<G_{BS}>_a$ given in Ref. 5. The subscripts a in θ_a^* and $<G_{BS}>_a$ indicate the particle species. The geometric factor $<G_{BS}>_a$ depends on the collisionality of the species a.

In CHS plasmas, there is no net toroidal current ($I = 0$). The first term of θ_a^* can be neglected in the plasma core ($\rho < 0.5$), because the toroidal velocity is dominant in these plasmas, with the tangential neutral beam injected in the toroidal direction. For instance, the normalized geometric factor for ions, $<G_{BS}>_i/(J/\tau) = 0.076$ and 0.137 , $\tau\,(v_\phi/R)/(v_\theta/r) = 0.3$ and 0.2 for $\rho = 0.3$ and 0.5, respectively in the plasma with $R_{ax} = 94.9$ cm. Thus, the parallel viscosity of ions given by Eq. (1) is simplified as

$$\langle \vec{B} \cdot \nabla \cdot \pi_i \rangle \approx \mu_i J \langle \vec{U}_i \cdot \nabla \phi \rangle = \left(\frac{2 n_i m_i \sqrt{2eT_i/m_i}\, v_\phi J}{\lambda_{PL} R} \right) \tag{1}$$

where, n_i, m_i, and T_i are ion density, mass and temperature, respectively. In CHS, ions are in the plateau collisionality regime and the viscosity coefficient μ_i is given by $2n_i m_i(2eT_i/m_i)^{1/2}/\lambda_{PL}$ and λ_{PL} is defined in Ref 5 as,

$$\frac{1}{\lambda_{PL}} \equiv \left(\frac{\sqrt{\pi}(J + \tau I)}{2\langle B^2\rangle}\right)\left\langle(\hat{\mathbf{n}}\bullet\nabla\mathbf{B})\sum_{mn}\frac{1}{|m\tau + n|}\left(\frac{1}{\mathbf{B}}\hat{\mathbf{n}}\bullet\nabla\mathbf{B}\right)_{mn}\exp^{i(m\theta + n\phi)}\right\rangle \quad (2)$$

where $\hat{\mathbf{n}}$ is normalized vector in the direction of magnetic field and m and n is poloidal and toroidal period number. Here we define a parallel viscosity coefficient for the toroidal flow, $\mu_{||}$ as

$$\mu_{||} \equiv \frac{\langle\vec{\mathbf{B}}\bullet\nabla\bullet\pi_i\rangle}{Bm_i n_i v_\phi} = \frac{2\sqrt{2eT_i/m_i}J}{\lambda_{PL}RB} \quad (3)$$

These values are closely related with the three dimensional magnetic field structure. In the large aspect ratio limit, it is simplified to $\mu_{||} = \pi^{1/2}\gamma^2(R/n)(2eT_i/m_i)^{1/2}$ with the modulation of the magnetic field modulation strength, γ, and the toroidal period number, n. The modulation of the magnetic field strength, γ, is defined as $\gamma^2 = \langle(\partial B/\partial s)^2\rangle/B^2$, where s is the length along the magnetic field line and $\langle\rangle$ is a flux surface average operator.

Figure 2 shows neoclassical parallel viscosity coefficient profiles calculated from magnetic structure including finite β effect in the plateau regime in CHS. Parallel viscosity coefficient increases very rapidly towards the plasma edge, which gives strong damping of toroidal rotation velocity, regardless of the position of the vacuum magnetic axis, $R_{ax.}$ As the magnetic axis is shifted outward, the parallel viscosity coefficient increases even near the plasma center. The increase of parallel viscosity coefficient by shifting the plasma from 89.9 cm, where there is negligible ripple, to 97.4 cm, where the helical ripple is more than 2 %, is one order of magnitude near the plasma center.

The parameter dependence of the viscosity coefficient is studied by changing the field ripple to check whether it is neoclassical or not. The damping of toroidal rotation velocity due to charge exchange loss can be neglected except at the plasma periphery. Here we introduce the effective viscosity coefficient μ_{eff} (1/s) as an indication of how strong the damping of central velocity is by parallel and perpendicular viscosities, $n_i m_i \mu_{\parallel} v_\phi$, and $-n_i m_i \mu_{\perp} \nabla^2 v_\phi$ in the plasma, where $\mu_{\parallel}$ (1/s) and $\mu_{\perp}$ (m^2/s) are parallel and perpendicular viscosity coefficients, respectively. Effective viscosity coefficient μ_{eff} is defined as $\mu_{eff}^{-1} = v_\phi(0) m_i n_e(0)/f_{NBI}(0)$, where $f_{NBI}(0)R$ is the torque due to neutral beam injection. If there is no perpendicular viscosity this effective viscosity coefficient is equal to the parallel viscosity coefficient , $\mu_{eff} = \mu_{\parallel}$. Figure 3 shows the inverse of the effective viscosity coefficient as a function of magnetic field ripple. The effective parallel viscosity coefficient μ_{eff} shows the γ^2 dependence as predicted by the neoclassical theory in the region where the neoclassical parallel viscosity becomes dominant, $\gamma > 0.2$. When the modulation of B decreases below 0.2, the neoclassical parallel viscosity becomes small and anomalous perpendicular viscosity, becomes dominant. The anomalous perpendicular viscosity coefficient, $\mu_{\perp}$, to fit the measured data is 2 m^2/s.

Since the plasma is in the plateau regime, the neoclassical parallel viscosity coefficient is independent of collisionality (electron density or ion temperature) except for v_{th} in formula (1). In order to check, the effective viscosity coefficient is measured at various densities. In this density scan, ion temperature was more or less constant. As seen in Fig. 4, the effective viscosity coefficient shows at most only weak dependence on the electron density, when the modulation of B is large (γ =

$0.42 m^{-1}$) and neoclassical parallel viscosity is dominant. However, when the modulation of B is small ($\gamma = 0.12 m^{-1}$) and neoclassical parallel viscosity is negligible, the effective viscosity coefficient has strong dependence on electron density. This density dependence is a feature of anomalous transport, because strong density dependence is also observed in the energy transport which is governed by anomalous transport.

The parallel viscosity coefficient derived from the toroidal rotation velocity shows good agreement with neoclassical parallel viscosity coefficient calculated with 3 dimensional magnetic structure, when the perpendicular viscosity with the coefficient, $\mu_{\perp}$, of 2 m^2/s is added to the neoclassical viscosities.

References

1) K.Ida and S.Hidekuma, Rev. Sci. Instrum. 60 (1989) 876.

2) K.C.Shaing, and J.D.Callen, Phys. Fluids 26 (1983) 1526.

3) K.Ida, Y.Yamada, H.Iguchi, K.Itoh, and CHS Group, Phys Rev. Lett. 67 (1991) 58.

4) N.Nakajima, M.Okamoto, and M.Fujiwara, Kakuyugo-kenkyu 68 (1992) 503.

5) K.Y.Watanabe, N.Nakajima, M.Okamoto, K.Yamazaki, Y.Nakamura, and M.Wakatani, Nucl. Fusion 35 (1995) 335.

Figure Captions

Fig.1. Radial profile of toroidal rotation velocity measured in CHS torsatron/heliotron for the vacuum magnetic axis of R_{ax} = 89.9, 94.9, 97.4 cm.

Fig.2. Radial profile of parallel viscosity coefficient in CHS torsatron/heliotron for the vacuum magnetic axis of R_{ax} = 89.9, 94.9, 97.4 cm.

Fig.3 Inverse of effective viscosity coefficient as a function of magnetic field modulation strength γ with the prediction with neoclassical parallel viscosity, $n_i m_i \mu_{\parallel} v_\phi$, and neoclassical parallel viscosity plus anomalous perpendicular viscosity, $n_i m_i \mu_{\parallel} v_\phi - n_i m_i \mu_\perp \nabla^2 v_\phi$ ($\mu_\perp = 2 m^2/s$), in CHS torsatron/heliotron.

Fig.4 Inverse of effective viscosity coefficient as a function of line averaged density.

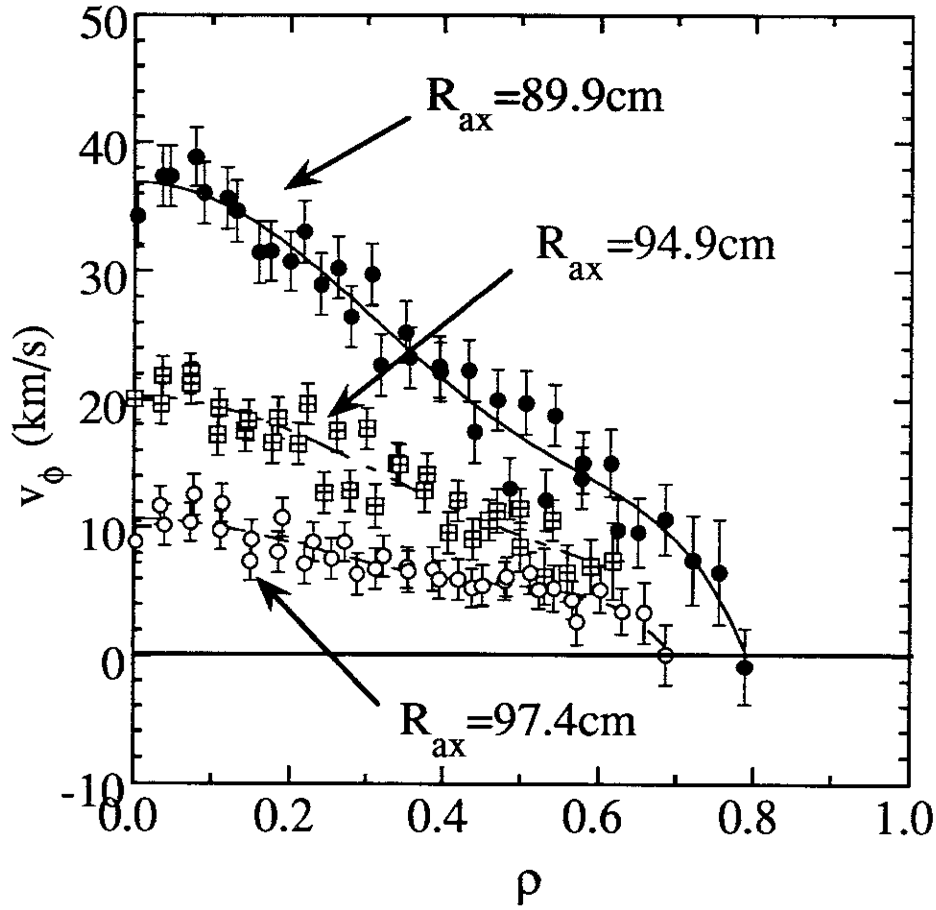

50
40
30
20
10
0
-10
0.0
0.2
0.4
0.6
0.8
1.0
ρ
v_φ (km/s)
R_ax=89.9cm
R_ax=94.9cm
R_ax=97.4cm

Figure 1

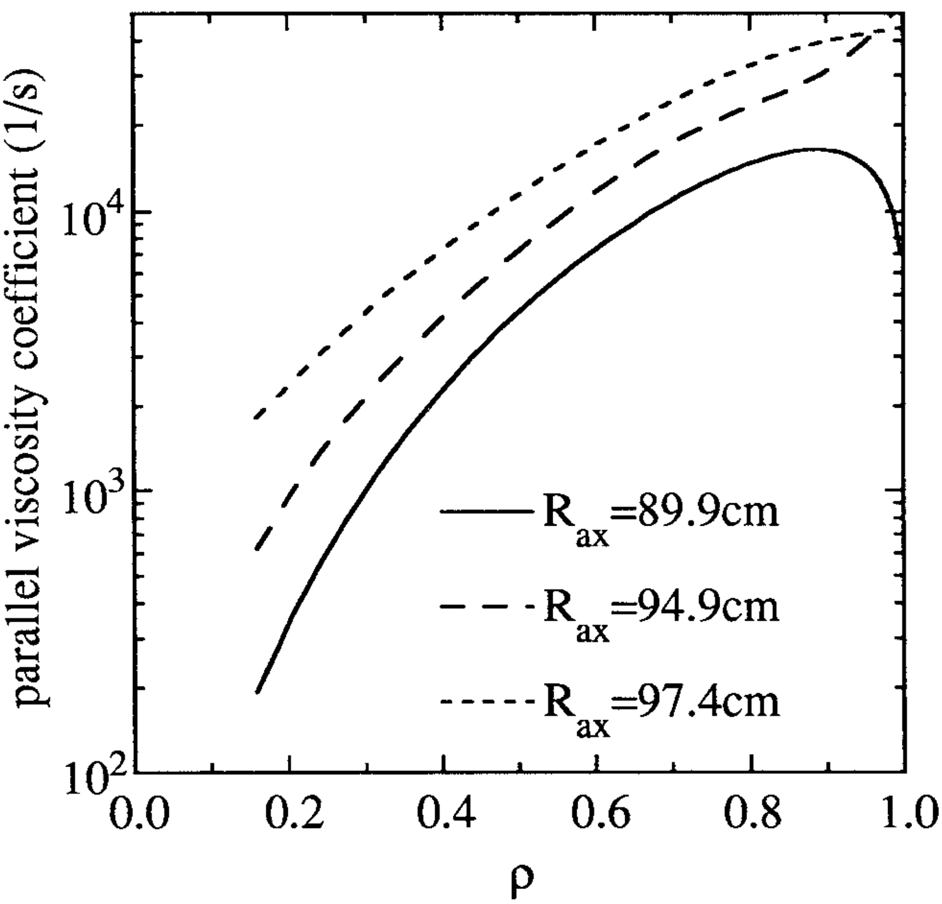
parallel viscosity coefficient (1/s)
10^4
10^3
10^2
0.0
0.2
0.4
0.6
0.8
1.0
ρ
R_{ax}=89.9cm
R_{ax}=94.9cm
R_{ax}=97.4cm

Figure 2

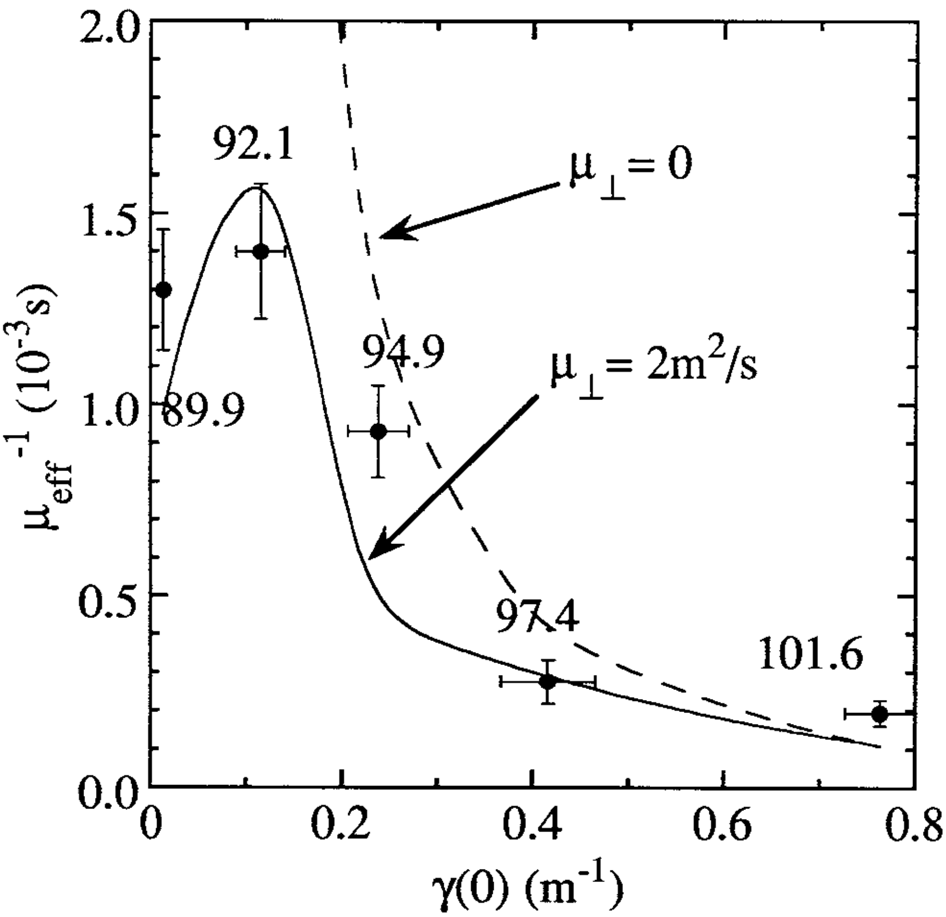

2.0
1.5
1.0
0.5
0.0
0
0.2
0.4
0.6
0.8
92.1
$\mu_\perp = 0$
94.9
$\mu_\perp = 2m^2/s$
89.9
97.4
101.6
μ_{eff}^{-1} (10^{-3}s)
γ(0) (m^{-1})

Figure 3

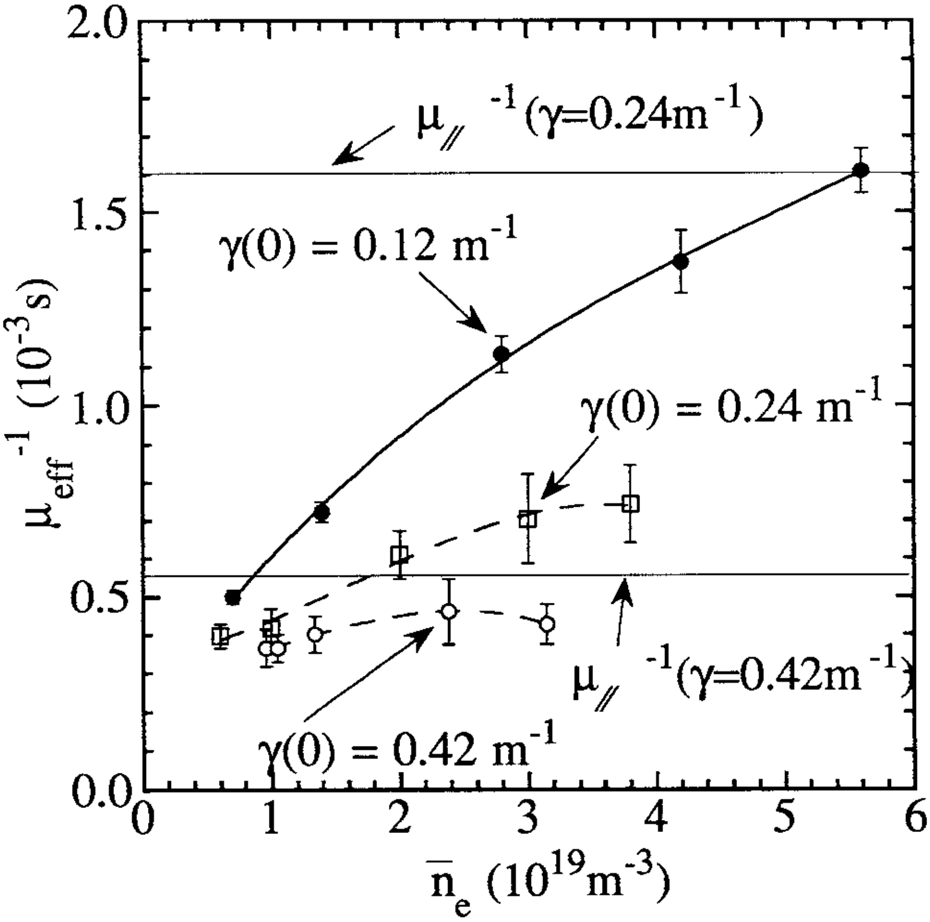

2.0
1.5
1.0
0.5
0.0
0
1
2
3
4
5
6
μ// -1(γ=0.24m-1)
γ(0) = 0.12 m-1
γ(0) = 0.24 m-1
μ// -1(γ=0.42m-1)
γ(0) = 0.42 m-1
μeff -1 (10-3s)
ne (1019m-3)

Figure 4

Recent Issues of NIFS Series

NIFS-364 H. Sugama and W. Horton
Entropy Production and Onsager Symmetry in Neoclassical Transport Processes of Toroidal Plasmas; July 1995

NIFS-365 K. Itoh, S.-I. Itoh, A. Fukuyama and M. Yagi,
On the Minimum Circulating Power of Steady State Tokamaks; July 1995

NIFS-366 K. Itoh and Sanae-I. Itoh,
The Role of Electric Field in Confinement; July 1995

NIFS-367 F. Xiao and T. Yabe,
A Rational Function Based Scheme for Solving Advection Equation; July 1995

NIFS-368 Y. Takeiri, O. Kaneko, Y. Oka, K. Tsumori, E. Asano, R. Akiyama, T. Kawamoto and T. Kuroda,
Multi-Beamlet Focusing of Intense Negative Ion Beams by Aperture Displacement Technique; Aug. 1995

NIFS-369 A. Ando, Y. Takeiri, O. Kaneko, Y. Oka, K. Tsumori, E. Asano, T. Kawamoto, R. Akiyama and T. Kuroda,
Experiments of an Intense H- Ion Beam Acceleration; Aug. 1995

NIFS-370 M. Sasao, A. Taniike, I. Nomura, M. Wada, H. Yamaoka and M. Sato,
Development of Diagnostic Beams for Alpha Particle Measurement on ITER; Aug. 1995

NIFS-371 S. Yamaguchi, J. Yamamoto and O. Motojima;
A New Cable -in conduit Conductor Magnet with Insulated Strands; Sep. 1995

NIFS-372 H. Miura,
Enstrophy Generation in a Shock-Dominated Turbulence; Sep. 1995

NIFS-373 M. Natsir, A. Sagara, K. Tsuzuki, B. Tsuchiya, Y. Hasegawa, O. Motojima,
Control of Discharge Conditions to Reduce Hydrogen Content in Low Z Films Produced with DC Glow; Sep. 1995

NIFS-374 K. Tsuzuki, M. Natsir, N. Inoue, A. Sagara, N. Noda, O. Motojima, T. Mochizuki, I. Fujita, T. Hino and T. Yamashina,
Behavior of Hydrogen Atoms in Boron Films during H_2 and He Glow Discharge and Thermal Desorption; Sep. 1995

NIFS-375 U. Stroth, M. Murakami, R.A. Dory, H. Yamada, S. Okamura, F. Sano and T. Obiki,
Energy Confinement Scaling from the International Stellarator Database;

Sep. 1995

NIFS-376 S. Bazdenkov, T. Sato, K. Watanabe and The Complexity Simulation Group,
Multi-Scale Semi-Ideal Magnetohydrodynamics of a Tokamak Plasma; Sep. 1995

NIFS-377 J. Uramoto,
Extraction of Negative Pionlike Particles from a H2 or D2 Gas Discharge Plasma in Magnetic Field; Sep. 1995

NIFS-378 K. Akaishi,
Theoretical Consideration for the Outgassing Characteristics of an Unbaked Vacuum System; Oct. 1995

NIFS-379 H. Shimazu, S. Machida and M. Tanaka,
Macro-Particle Simulation of Collisionless Parallel Shocks; Oct. 1995

NIFS-380 N. Kondo and Y. Kondoh,
Eigenfunction Spectrum Analysis for Self-organization in Dissipative Solitons; Oct. 1995

NIFS-381 Y. Kondoh, M. Yoshizawa, A. Nakano and T. Yabe,
Self-organization of Two-dimensional Incompressible Viscous Flow in a Friction-free Box; Oct. 1995

NIFS-382 Y.N. Nejoh and H. Sanuki,
The Effects of the Beam and Ion Temperatures on Ion-Acoustic Waves in an Electron Beam-Plasma System; Oct. 1995

NIFS-383 K. Ichiguchi, O. Motojima, K. Yamazaki, N. Nakajima and M. Okamoto
Flexibility of LHD Configuration with Multi-Layer Helical Coils; Nov. 1995

NIFS-384 D. Biskamp, E. Schwarz and J.F. Drake,
Two-dimensional Electron Magnetohydrodynamic Turbulence; Nov. 1995

NIFS-385 H. Kitabata, T. Hayashi, T. Sato and Complexity Simulation Group,
Impulsive Nature in Collisional Driven Reconnection; Nov. 1995

NIFS-386 Y. Katoh, T. Muroga, A. Kohyama, R.E. Stoller, C. Namba and O. Motojima,
Rate Theory Modeling of Defect Evolution under Cascade Damage Conditions:The Influence of Vacancy-type Cascade Remnants and Application to the Defect Production Chracterization by Microstructural Analysis; Nov. 1995

NIFS-387 K. Araki, S. Yanase and J. Mizushima,
Symmetry Breaking by Differential Rotation and Saddle-node Bifurcation of the Thermal Convection in a Spherical Shell; Dec. 1995

NIFS-388 V.D. Pustovitov.
Control of Pfirsch-Schluter Current by External Poloidal Magnetic Field in Conventional Stellarators. Dec 1995

NIFS-389 K. Akaishi,
On the Outgassing Rate Versus Time Characteristics in the Pump-down of an Unbaked Vacuum System; Dec. 1995

NIFS-390 K.N. Sato, S. Murakami, N. Nakajima, K. Itoh,
Possibility of Simulation Experiments for Fast Particle Physics in Large Helical Device (LHD); Dec. 1995

NIFS-391 W.X.Wang, M. Okamoto, N. Nakajima, S. Murakami and N. Ohyabu,
A Monte Carlo Simulation Model for the Steady-State Plasma in the Scrape-off Layer; Dec. 1995

NIFS-392 Shao-ping Zhu, R. Horiuchi, T. Sato and The Complexity Simulation Group,
Self-organization Process of a Magnetohydrodynamic Plasma in the Presence of Thermal Conduction; Dec. 1995

NIFS-393 M. Ozaki, T. Sato, R. Horiuchi and the Complexity Simulation Group
Electromagnetic Instability and Anomalous Resistivity in a Magnetic Neutral Sheet; Dec. 1995

NIFS-394 K. Itoh, S.-I Itoh, M. Yagi and A. Fukuyama,
Subcritical Excitation of Plasma Turbulence; Jan. 1996

NIFS-395 H. Sugama and M. Okamoto, W. Horton and M. Wakatani,
Transport Processes and Entropy Production in Toroidal Plasmas with Gyrokinetic Eletromagnetic Turbulence; Jan. 1996

NIFS-396 T. Kato, T. Fujiwara and Y. Hanaoka,
X-ray Spectral Analysis of Yohkoh BCS Data on Sep. 6 1992 Flares - Blue Shift Component and Ion Abundances -; Feb. 1996

NIFS-397 H. Kuramoto, N. Hiraki, S. Moriyama, K. Toi, K. Sato, K. Narihara, A. Ejiri, T. Seki and JIPP T-IIU Group,
Measurement of the Poloidal Magnetic Field Profile with High Time Resolution Zeeman Polarimeter in the JIPP T-IIU Tokamak; Feb. 1996

NIFS-398 J.F. Wang, T. Amano, Y. Ogawa, N. Inoue,
Simulation of Burning Plasma Dynamics in ITER; Feb. 1996

NIFS-399 K. Itoh, S-I. Itoh, A. Fukuyama and M. Yagi,
Theory of Self-Sustained Turbulence in Confined Plasmas; Feb. 1996

NIFS-400 J. Uramoto,
A Detection Method of Negative Pionlike Particles from a H2 Gas

Descharge Plasma; Feb. 1996

NIFS-401 K.Ida, J.Xu, K.N.Sato, H.Sakakita and JIPP TII-U group,
Fast Charge Exchange Spectroscopy Using a Fabry-Perot Spectrometer in the JIPP TII-U Tokamak; Feb. 1996

NIFS-402 T. Amano,
Passive Shut-Down of ITER Plasma by Be Evaporation; Feb. 1996

NIFS-403 K. Orito,
A New Variable Transformation Technique for the Nonlinear Drift Vortex; Feb. 1996

NIFS-404 T. Oike, K. Kitachi, S. Ohdachi, K. Toi, S. Sakakibara, S. Morita, T. Morisaki, H. Suzuki, S. Okamura, K. Matsuoka and CHS group;
Measurement of Magnetic Field Fluctuations near Plasma Edge with Movable Magnetic Probe Array in the CHS Heliotron/Torsatron; Mar. 1996

NIFS-405 S.K. Guharay, K. Tsumori, M. Hamabe, Y. Takeiri, O. Kaneko, T. Kuroda,
Simple Emittance Measurement of H- Beams from a Large Plasma Source; Mar. 1996

NIFS-406 M. Tanaka and D. Biskamp,
Symmetry-Breaking due to Parallel Electron Motion and Resultant Scaling in Collisionless Magnetic Reconnection; Mar. 1996

NIFS-407 K. Kitachi, T. Oike, S. Ohdachi, K. Toi, R. Akiyama, A. Ejiri, Y. Hamada, H.Kuramoto, K. Narihara, T. Seki and JIPP T-IIU Group,
Measurement of Magnetic Field Fluctuations within Last Closed Flux Surface with Movable Magnetic Probe Array in the JIPP T-IIU Tokamak; Mar. 1996

NIFS-408 K. Hirose, S. Saito and Yoshi.H. Ichikawa
Structure of Period-2 Step-1 Accelerator Island in Area Preserving Maps; Mar. 1996

NIFS-409 G.Y.Yu, M. Okamoto, H. Sanuki, T. Amano,
Effect of Plasma Inertia on Vertical Displacement Instability in Tokamaks; Mar. 1996

NIFS-410 T. Yamagishi,
Solution of Initial Value Problem of Gyro-Kinetic Equation; Mar. 1996

NIFS-411 K. Ida and N. Nakajima,
Comparison of Parallel Viscosity with Neoclassical Theory; Apr. 1996